Annotation and quantification of N-acyl homoserine lactones implied in bacterial quorum sensing by supercritical-fluid chromatography coupled with high-resolution mass spectrometry

Thi Phuong Thuy Hoang, Morgane Barthélemy, Raphaël Lami, Didier Stien, Véronique Eparvier, David Touboul

Annotation and quantification of *N*-acyl homoserine lactones implied in bacterial quorum-sensing by Supercritical-Fluid Chromatography coupled to High-Resolution Mass Spectrometry (SFC-HRMS)

Thi Phuong Thuy Hoang[1], Morgane Barthélemy[1], Raphaël Lami[2], Didier Stien[2], Véronique Eparvier[1], David Touboul[1]

[1]*Institut de Chimie des Substances Naturelles, CNRS UPR 2301, Université Paris-Saclay, Avenue de la Terrasse, Gif-sur-Yvette, France*
[2]*Sorbonne Université, CNRS, Laboratoire de Biodiversité et Biotechnologies Microbiennes (LBBM), USR3579, Observatoire Océanologique de Banyuls-sur-Mer, France*

Correspondance to: David Touboul, Institut de Chimie des Substances Naturelles, CNRS UPR 2301, Univ. Paris-Sud, Université Paris-Saclay, Avenue de la Terrasse, 91198 Gif-sur-Yvette, France. Email: david.touboul@cnrs.fr

Abstract

In recent years, supercritical-fluid chromatography (SFC) using CO_2 as the mobile phase is expanding in the research laboratory and industry since it is considered as a green analytical method. This technic offers numerous advantages such as good separation and sensitive detection, short analysis times and stability for analytes. In this study, a method for quantification of lipids, called *N*-acyl homoserine lactones (AHLs), signal molecules responsible of cell-to-cell communication initially discovered in the kingdom of bacteria, by SFC coupled to high-resolution mass spectrometry (SFC-HRMS) was developed. Optimization of SFC condition together with MS ionization settings to reach the best separation and sensitivity were investigated. The established optimal analysis conditions allow quantification of up to 30 AHLs in a single run within 16 min with excellent linearity (R^2 >0.998) as well as sensitivity (pg level). This method was then applied to study AHLs production of one gram-negative endophytic bacterium *Paraburkholderia* sp. BSNB-0670. Nineteen known AHLs were detected, and nine abundant HSLs were quantified. To further investigate the production of uncommon AHLs, a molecular networking approach was conducted based on SFC-HRMS/MS data. This led to additionally identify four unknown AHLs annotated as *N*-3-hydroxy-dodecanoylol homoserine lactone, *N*-3-hydroxy-dodecadienoyl homoserine lactone (3-OH-C12:2-HSL) and two *N*-3-oxo-dodecenoyl homoserine lactone (3-oxo-C12:1-HSLs).

Key words

Supercritical-Fluid Chromatography, *N*-acyl homoserine lactone, quorum sensing, quantification, molecular networking

Introduction

Quorum sensing (QS) is a regulatory system that has been characterized in many diverse types of bacteria and responsible for controlling gene expression when increasing cell density by secreting hormone-like compounds called autoinducers [1, 2]. The bacterial group behavior could consequently be regulated such as cell division, production of secondary metabolites and virulence factors, the appearance of bioluminescence and biofilm formation [3]. There are three main bacterial QS systems which use different types of autoinducers: the LuxI/LuxR-type QS in Gram-negative bacteria using lipids called *N*-acyl homoserine lactones (AHLs), oligopeptide-two-component-type QS in Gram-positive using small peptides, and luxS-encoded autoinducer 2 (AI-2) QS constituting an interspecies communication system [4]. Furthermore, quorum sensing also involves interkingdom signaling described as the symbiont-symbiont and host-symbiont interactions [5]. QS signaling is employed by several important bacterial pathogens so regulation of bacterial quorum sensing systems to inhibit pathogenesis is a promising approach to antimicrobial therapy without engendering bacterial resistance [6]. Among described signal molecules, the *N*-acyl homoserine lactone (AHL) family (Fig. 1) has been the most intensively investigated. The AHLs consist of a fatty acid coupled with homoserine lactone and differ in the nature of the acyl side chain (length, degree of unsaturation) and substitution at position 3 (unsubstituted or substituted by a carbonyl or hydroxyl group) [7]. To date, more than twenty AHLs typically having the acyl chain length from 4 to 19 [8] carbons have been described. Identification and quantification of AHLs are helpful to determine methods to monitor, predict and regulate bacterial gene expression [9]. There are two principal types of quantification method developed for AHLs based on biological (bacterial biosensors) or chemical method. Bacterial biosensors allow the detection of AHL *in situ* but in a limited range of AHL structures since each biosensor strain responses to only particular AHLs [10]. Furthermore, this technique is limited when the concentration of AHLs is below the activation threshold of the biosensor and the AHL quantification is generally inaccurate [10, 11]. The second one such as chromatography coupled to mass spectrometry is more efficient to analyze complex mixtures of AHLs. Different methods were developed for identification and quantification of AHLs such as gas chromatography-mass spectrometry (GC-MS) [12] which was developed for the quantification of the 3-oxo-HSLs based on the conversion of these compounds to their pentafluorobenzyloxime derivatives in a study of Charlton *et al*. [13]. In 2005, Frommberger *et al.* also developed a quantitative, specific, and sensitive method for the determination of AHLs under their hydrolysis form by capillary zone electrophoresis-mass spectrometry [14]. The liquid chromatography coupled to mass spectrometry (LC-MS or LC-MS/MS) was also widely employed to determine AHLs with high mass resolution and mass accuracy [9, 10, 15, 16]. Another method named matrix-assisted laser desorption/ionization time-of-flight mass spectrometry (MALDI-TOF MS) was tested to analyze AHLs leading a fast, straightforward and highly sensitive method with very low limits of quantification from one to five pmol but did not allow the separation of isomers [17]. Over the last few years, supercritical-fluid chromatography (SFC) has been widely developed and applied to analyze various natural products [18, 19] because this green technique exhibits numerous advantages such as low toxicity for users, low consumption of organic solvent, high-speed and high-resolution separation [20, 21]. Therefore, it would be interesting to investigate the capacity of AHLs detection and quantification by this method.

In this study, we have optimized and validated a fast and sensitive SFC-HRMS method for the identification and quantification of up to 30 AHLs in a single run. This established method was successfully applied to determine AHLs produced by the Gram negative bacterium *Paraburkholderia* sp. BSNB-0670 [22]. Additionally, further investigation of the production of uncommon AHLs was carried out by a molecular networking workflow after SFC-HRMS/MS analysis.

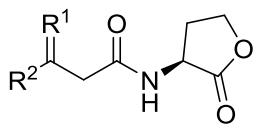

R^1	
-H	Non-oxidized AHL
-H,-OH	3-Hydroxy-AHL
=O	3-Oxo-AHL

Fig. 1 Chemical structure of AHLs

Materials and Methods

Chemicals

Carbon dioxide (purity ≥ 99.7 %) was purchased from Air Liquide (Grigny, France). Methanol (HPLC grade) was purchased from J.T.Baker (Center Valley, PA, USA), ethanol absolute anhydrous (HPLC-Isocratic grade) from Carlo Erba (Val de Reuil, France), 2-propanol (LC-MS grade) from Fisher Scientific (Illkirch, France), acetonitrile (ultra-gradient HPLC grade) from J.T.Baker (Center Valley, PA, USA), dichloromethane (stabilized with ethanol) from Carlo Erba (Val de Reuil, France). Ammonium acetate (LC-MS grade) was purchased from Sigma-Aldrich (Saint-Quentin Fallavier, France).

Standards

N-acyl homoserine lactones: *N*-acetyl-L-homoserine lactone (C2-HSL), *N*-butanoyl-DL-homoserine lactone (C4-HSL), *N*-3-hydroxy-butanoyl-L-homoserine lactone (3-OH-C4-HSL), *N*-hexanoyl-L-homoserine lactone (C6-HSL), *N*-3-oxo-hexanoyl-L-homoserine lactone (3-oxo-C6-HSL), *N*-heptanoyl- L- homoserine lactone (C7-HSL), *N*-octanoyl-L-homoserine lactone (C8-HSL), *N*-3-oxo-octanoyl-L-homoserine lactone (3-oxo-C8-HSL), *N*-nonanoyl-L-homoserine lactone (C9-HSL), *N*-3-hydroxy-octanoyl-L-homoserine lactone (3-OH-C8-HSL), *N*-(*p*-Coumaroyl)-L-homoserine lactone (*N*-(*p*-Coumaroyl)-L-HSL), *N*-decanoyl-DL-homoserine lactone (C10-HSL), *N*-3-oxo-decanoyl-L-homoserine lactone (3-oxo-C10-HSL), *N*-undecanoyl-L-homoserine lactone (C11-HSL), *N*-3-hydroxy-decanoyl-L-homoserine lactone (3-OH-C10-HSL), *N*-dodecanoyl-DL-homoserine lactone (C12-HSL), *N*-3-oxo-dodecanoyl-L-homoserine lactone (3-oxo-C12-HSL), *N*-3-hydroxy-dodecanoyl-DL-homoserine lactone (3-OH-C12-HSL), *N*-tridecanoyl-L-homoserine lactone (C13-HSL), *N*-*cis*-tetradec-9-enoyl-L-homoserine lactone (C14:1-Δ^9-*cis*-HSL), *N*-tetradecanoyl-L-homoserine lactone (C14-HSL), *N*-*cis*-3-oxo-tetradec-7-enoyl-L-homoserine lactone (3-oxo-C14:1-Δ^7-*cis*-HSL), *N*-3-oxo-tetradecanoyl-L-homoserine lactone (3-oxo-C14-HSL), *N*-3-hydroxy-tetradecanoyl-L-homoserine lactone (3-OH-C14-HSL), *N*-pentadecanoyl-L-homoserine lactone (C15-HSL), *N*-*cis*-hexadec-9-enoyl-L-homoserine lactone (C16:1-Δ^9-*cis*-HSL), *N*-hexadecanoyl-L-homoserine lactone (C16-HSL), *N*-*cis*-3-oxo-hexadec-11-enoyl-L-homoserine lactone (3-oxo-C16:1-Δ^{11}-*cis*-HSL), *N*-3-oxo-hexadecanoyl-L-homoserine lactone (3-oxo-C16-HSL), *N*-*cis*-octadec-9-enoyl-L-homoserine lactone (C18:1-Δ^9-*cis*-HSL) and *N*-octadecanoyl-L-homoserine lactone (C18-HSL) were obtained from Sigma-Aldrich (Saint-Quentin Fallavier, France) and Interchim (Montluçon, France).

The stock solutions at 1 g.L^{-1} were prepared in acetonitrile (CH_3CN) except for C4-HSL (0.50 g.L^{-1}), C13-HSL (0.50 g.L^{-1}), C15-HSL (0.67 g.L^{-1}), C16-HSL (0.50 g.L^{-1}) and C18-HSL (0.67 g.L^{-1}). C15-HSL, C16-HSL and C18-HSL were not well solubilized in pure acetonitrile so they were prepared in CH_3CN/CH_2Cl_2 2:1, 1:1 and 2:1 (v/v), respectively. The solutions were kept at -20 °C in glass vials.

The mixture MixHSL_01 used for the column screening consisted of seven AHLs: C6-HSL, 3-oxo-C6-HSL, C8-HSL, 3-oxo-C8-HSL, C10-HSL, 3-oxo-C10-HSL and 3-OH-C10-HSL (14.3 mg.L^{-1}).

The secondary mixture MixHSL_02 employed for optimizing the SFC separation consisted of fourteen AHLs: C6-HSL, 3-oxo-C6-HSL, C8-HSL, 3-oxo-C8-HSL, C10-HSL, 3-oxo-C10-HSL, 3-OH-C10-HSL, C15-HSL, C16:1-Δ^9-*cis*-HSL, C16-HSL, 3-oxo-C16:1-Δ^{11}-*cis*-HSL, 3-oxo-C16-HSL, C18:1-Δ^9-*cis*-HSL and C18-HSL (23.8 mg.L^{-1}) except for C15-HSL (15.95 mg.L^{-1}), C16-HSL (11.90 mg.L^{-1}) and C18-HSL (15.95 mg.L^{-1}).

The mixture of 30 AHLs used for the calibration curves was prepared at different concentrations: 10 µL of each stocked solution were mixed giving MixHSL_C0. This solution was then diluted 2, 4, 10, 20, 40, 100, 200 and 400 times giving MixHSL_C2, C4, C10, C20, C40, C100, C200, C400, respectively. C2-HSL was used as an internal standard at a fixed concentration of 0.65 $mg.L^{-1}$.

Bacterial Strains, Fermentation, Extraction and Sample Preparation

The endophytic bacterium *Paraburkholderia* sp. BSNB-0670 was isolated from an amazonian palm tree *Astrocaryum sciophilum* sampled in French Guiana in Piste de Saint-Elie, Sinnamary [22]. It was identified using nucleotides sequencing of the rDNA 16S region (GenBank accession no. MK643275). The strain is stored at the Institut de Chimie des Substances Naturelles under the identification code BSNB-0670.

Cultivation of bacterial strain was carried out in Petri dishes (10 cm diameter) using potato dextrose agar at 28 °C. After one week of cultivation, the whole fermented culture was extracted by 100 mL of CH_2Cl_2 at room temperature. Mixtures of bacteria and agar layer were cut, gently shaken for 24 hours then filtered on cottons. The culture residues were rinsed by 100 mL of CH_2Cl_2 and filtered on cotton. Organic phases were combined and evaporated to dryness resulting in crude extract. Samples were re-suspended in MeOH/CH_2Cl_2 1:1 (v/v) at a final concentration of 1 $mg.mL^{-1}$ before SFC-MS and SFC-MS/MS analyses.

Supercritical Fluid Chromatography (SFC)

Analyses were performed with a 1260 Infinity Analytical SFC system (Agilent Technologies, Waldbronn, Germany) consisted of the Aurora module and an “LC-like” system. This system was equipped with a thermostated autosampler (kept at 5 °C) with a 1.2 µL injection loop and two thermostated column compartments that can contain up to eight columns.

Seven columns were selected for the screening of the stationary phase: Torus Acquity UPC^2 1-aminoanthracene (1-AA) (50 mm × 2.1 mm, 1.7 µm), TorusAcquity UPC^2 diethylamine-bonded silica (DEA) (50 mm × 2.1 mm, 1.7 µm) and Acquity UPC^2 BEH 2-ethylpyridine (2-EP) (100 mm × 2.1 mm, 1.7 µm) purchased from Waters (Guyancourt, France); Hypercarb™ (100 mm × 2.1 mm, 5 µm) from Thermo Fisher Scientific (Courtaboeuf, France); Zorbax RX-Silica (Si) RRHT (100 mm × 2.1 mm, 1.8 µm), ZORBAX Eclipse Plus C18 - Rapid Resolution HT (C18) (150 mm × 2.1 mm, 1.8 µm) and Pursuit 3 pentafluorophenyl (PFP) (150 mm × 2mm, 3 µm) from Agilent Technologies (Massy, France). The Hypercarb™ stationary phase was selected for the quantification. For a better separation, a Hypercarb™ column (100 mm × 2.1 mm, 3 µm) purchased from Thermo Fisher Scientific (Courtaboeuf, France) was employed.

The mobile phase was composed of CO_2 (A) and co-solvent (B). For the screening of stationary phase, the mixture of MeOH/EtOH 1:1 v/v with 20 mM of ammonium acetate ($AcONH_4$) was employed as co-solvent. The flow rate was fixed at 1 $mL.min^{-1}$. Run time of 16 min was employed as follows: 0.0-1.5 min (1-5% B), 1.5-7.0 min (5-15% B), 7-10 min (15% B), 10-12 min (15-30% B), 12-13 min (30% B), 13-14 min (30-1% B), 14-16 min (1% B). The column oven was kept at 60 °C. The back-pressure regulator (BPR) was set at 130 bar and 60 °C.

To get the optimum SFC separation, the nature of co-solvent together with different values of column oven temperature (30, 40, 50 and 60 °C) and back-pressure regulator (BPR) (110, 130, 140 and 150 bar) were investigated.

SFC-HRMS Analysis

The SFC system was coupled to a quadrupole time-of-flight (QTOF) mass spectrometer 6540 Agilent (Agilent Technologies, Massy, France). The electrospray ionization ESI dual JetStream was employed for analysis because it offered a high ionization capacity of analytes. Experiments were carried out in positive

mode. Parameters were fixed with drying gas at 10 $L.min^{-1}$, nebulizer at 50 psi, sheath gas temperature at 350 °C, sheath gas flow at 11 $L.min^{-1}$, nozzle voltage at 1000 V, skimmer at 45 V, Oct 1 RF Vpp at 750 V. Other optimized parameters such fragmentor voltage, drying-gas temperature and the capillary Vcap were further investigated. MS scans were operated in full-scan mode from *m/z* 50 to *m/z* 1000 at 2 GHz resulting in a mass resolution of 25 000 at *m/z* 922. Two internal reference masses (purine, $C_5H_4N_4$, *m/z* 121.0509, and HP-921 [hexakis-(1*H*,1*H*,3*H*-tetrafluoro pentoxy)phosphazene], $C_{18}H_{18}O_6N_3P_3F_{24}$, *m/z* 922.0098) were purchased from Agilent (Agilent Technologies, Massy, France). Calibration solution was injected routinely resulted in mass accuracy below 5 ppm. The mass spectrometer was operated in full-scan mode. Recorded data were analyzed using MassHunter Workstation software (B.08.00). For each ion of interest, the extracted ion chromatogram (XIC) was calculated by selecting the theoretical *m/z* value with a selection window of 20 ppm. The mixture of MeOH/EtOH 1:1 (v/v) with 20 mM $AcONH_4$ was used as a make-up solvent which was pumped by a 1260 Infinity isocratic pump (Agilent Technologies, Massy, France) at a flow rate of 0.2 $mL.min^{-1}$. To avoid the freezing of the transfer line, a Caloratherm (Sandra Selerity Technologies, Kortrijk, Belgium) fixed at 60 °C was added before the ion source.

SFC-HRMS/MS Analysis

To determine if *Paraburkholderia* sp. BSNB-0670 produced AHLs with long side chain which could be eluted lately, run time of quantitative method was increased by extending the duration of the plateau at 55% of co-solvent B from 3 to 12 min. Source parameters and MS scans were set as above. The data-dependent MS/MS events were acquired on the five most intense ions detected in full-scan MS (five max precursors per cycle) above an absolute threshold of 1000 counts. Selected parent ions were fragmented at a fixed collision energy value of 15 eV and an isolation window of 1.3 amu. The mass range of precursor and fragment ion was set in the range *m/z* 50-1000.

Data Processing

The SFC-HRMS/MS raw data file was converted to *.mzXML file by using the MSConvert software. The MzXML file was subjected to MZmine 2.38 analysis [23]. The mass detection was performed using a centroid algorithm with a noise level of 100 for both MS level 1 and 2. The chromatogram builder was proceeded using ADAP (Automated Data Analysis Pipeline) algorithm [24] with following setting parameters: a minimum group size of scans of 2, a minimum group intensity threshold of 100, a minimum highest intensity of 100 and a *m/z* tolerance of 0.01 or 10 ppm. The chromatogram deconvolution was carried out employing the wavelets (ADAP) algorithm with following setting parameters: Signal-to-Noise ratio (S/N) threshold of 10, an intensity window SN, a minimum feature height of 1000, a coefficient/area threshold of 10, a peak duration range between 0.02 and 1.00, a retention time (RT) wavelet range between 0.02 and 0.20. The *m/z* and RT range for MS2 scan pairing were 0.02 Da and 0.5 min, respectively. Chromatograms were deisotoped using the isotopic peaks grouper algorithm with an *m/z* tolerance of 0.001 or 10 ppm, RT tolerance of 0.2 (absolute), maximum charge of 2 and the representative isotope used was the most intense. The adduct identification (Na^+, K^+, NH_4^+, ACN^+ (acetonitrile)) was carried out on the peak list with an RT tolerance of 0.05 min; *m/*z tolerance of 0.001 or 10 ppm; the maximum relative peak height of 50%. The found adducts were then removed from the peak list. The peak list was exported both as a *.mgf file and as a *.csv file (metadata). The calculation and visualization of the molecular network was performed by MetGem software [25]. The parameters were set as follow: *m/z* tolerance of 0.02, minimum matched peaks of 5, topK of 10, minimal cosine score value of 0.7 and maximum connected component size of 1000.

Method Validation

Specificity

The specificity of the method was performed to investigate the potential interferences occurred in acetonitrile used for the sample preparation. For this purpose, pure acetonitrile was analyzed and then compared to the calibration level. If there is no interfering peak at the retention times of AHL standards, the specificity of the methods will be validated.

Linearity

C2-HSL has not been isolated yet from bacterial extract so it was used as internal standard (IS) for the determination of calibration curves to correct for deviations of injection volume of the autosampler. Least-squares linear regressions were calculated based on the ratio between the peak area of the analyte and that of the IS as a function of the analyte concentration at nine different levels (0.040-32.26 $mg.L^{-1}$) in triplicate experiments. The slope, the *y*-intercept of the calibration curve as well as the coefficient of determination (R^2) were calculated for each standard.

LOD and LOQ

The limits of detection (LOD) and the limits of quantification (LOQ) were defined as the concentration with a signal-to-noise ratio (S/N) of 3 and 10, respectively [26].

Intra- and Inter-day Precision and Accuracy (Repeatability and Reproducibility)

To study intra-day precision, three calibration levels (low-C100, medium-C40 and high-C10, except for *N*-(*p*-Coumaroyl)-HSL which was measured at C2, C10 and C40 because of its limit of detection) were injected in triplicate in a single run. To study inter-day precision, this experiment using the medium concentration (MixHSL_C40) was repeated three times in three different days. The relative standard deviations (RSD), the coefficient of variations (%CV), the back-calculated concentrations as well as the accuracy were determined.

Recovery of Analytes from Medium

To determine the recovery of the extraction protocol, the standard solutions were spiked into bacterial culture media before extraction to have two final concentrations (low-C100 and high-C10 concentrations, considering 100% of recovery). The extraction process was conducted as described above. This experiment was carried out in triplicate for each standard level. After triplicate SFC-MS analyses, the recovery values were determined as peak area ratios between spiked extract and the standard solutions before extraction.

Application of the Validated Method

The validated method was used to determine AHLs produced by one gram-negative endophytic bacterium *Paraburkholderia* sp. BSNB-0670 isolated from an amazonian palm tree *Astrocaryum sciophilum*. Fermentation, extraction, sample preparation and analyses in triplicate were realized as described above. Each AHL was identified based on its retention time, the exact mass of $[M+H]^+$ ion together with the characteristic fragmentation ions compared with that of AHL standards. The quantification of different AHLs produced by the studied strain was performed based on established calibration curves.

Results and Discussion

Optimization of SFC Separation

SFC method was first optimized to reach an efficient separation of AHLs in a short time (less than 10 minutes). Different parameters were investigated such as the type of stationary phases, the mobile phase composition, the temperature of the column-compartment. Seven columns distributed in different sets of orthogonal chromatographic systems [27] were tested by using a standard mixture and a generic gradient.

A mixture containing seven typical AHLs, *i.e.* short and long chain with/without lateral hydroxyl groups, was used. Results presented in Fig. 2 show that these seven AHLs were co-eluted in the first minute of injection on the two columns PFP and C18. These AHLs were more retained (within five minutes) when using four other stationary phases DEA, RX-SIL, 2-EP and 1-AA but we still observed the co-elution of several peaks, indicating that these stationary phases were not selective enough for homoserine lactone separation. The Hypercarb™ column provided the best separation of all AHLs in the mixture within a reasonable time of 10 min. Although some chromatographic peaks were not sharp and symmetric, Hypercarb™ column was selected for further method improvement.

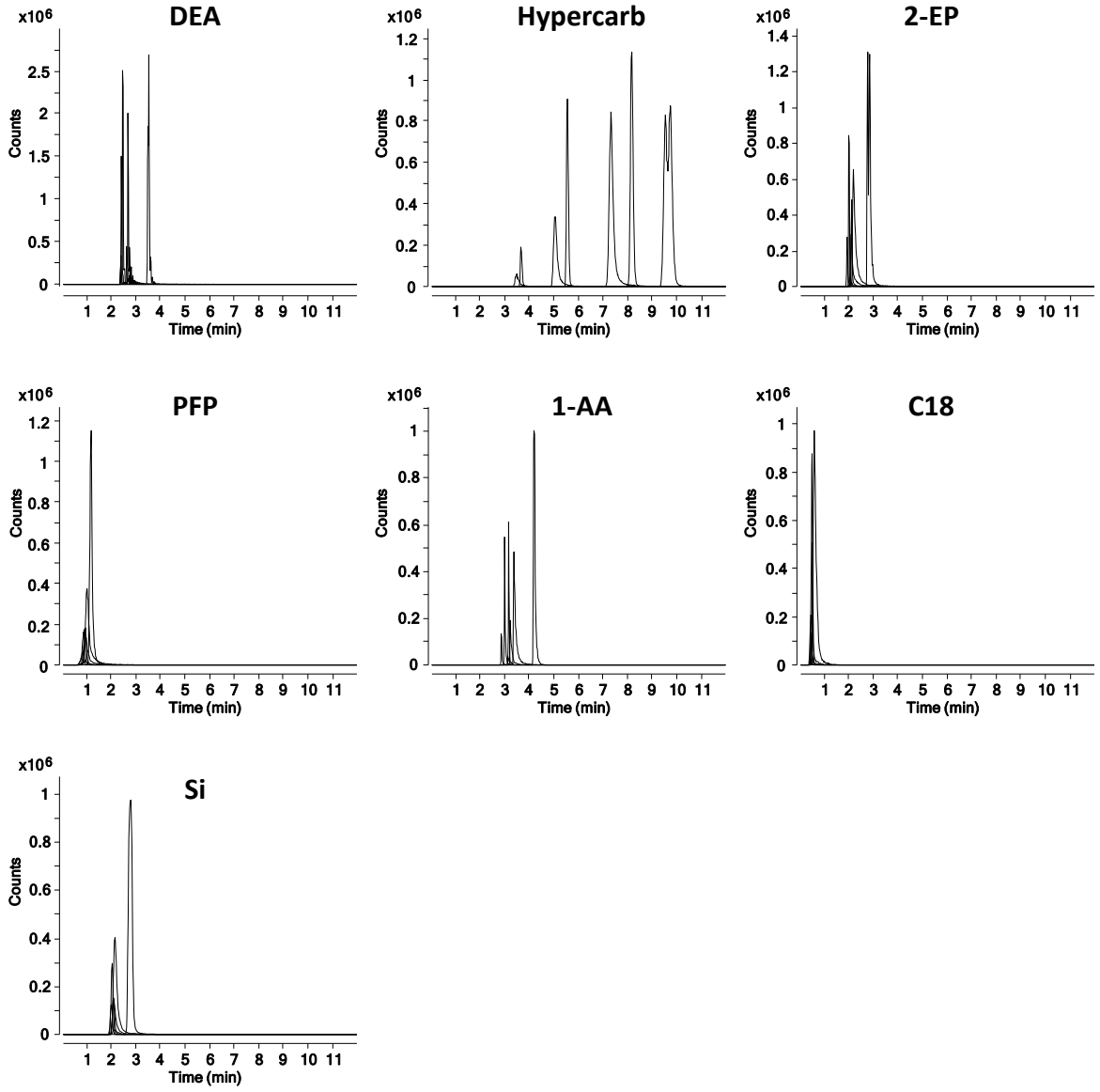

Fig. 2 Extracted ion chromatograms of seven homoserine lactones analyzed by SFC-MS with seven different stationary phases: DEA (diethylamine-bonded silica), Hypercarb, 2-EP (2-ethylpyridine-bonded silica), PFP (pentafluorophenyl-bonded silica), 1-AA (1-aminoanthracene-bonded silica), C18 (octadecyl carbon-bonded silica) and Si (pure silica); Elution: Mobile phase was CO_2 (A) with co-solvent (B) and solvent make-up using MeOH/EtOH 1:1 (v/v) with 20 mM of $AcONH_4$; flow rate 1 $mL.min^{-1}$; run time: 0.0-1.5 min (1-5% B), 1.5-7.0

min (5-15% B), 7-10 min (15% B), 10-12 min (15-30% B), 12-13 min (30% B), 13-14 min (30-1% B), 14-16 min (1% B); column oven at 60 °C; the back-pressure regulator (BPR) at 130 bar and 60 °C

To study the influence of mobile phase composition as well as its flow rate, a more complex mixture of standards containing 14 AHLs was prepared as described in the materials and methods section. When using the generic program to analyze it, the chromatographic peaks of seven AHLs from C6 to C10 were very large and showed poor peak symmetry. The other seven AHLs with long side-chain were not detected at all, suggesting either no elution from the column or weak ionization efficiency in the present conditions. The percent of co-solvent (MeOH/EtOH 1:1 with 20 mM $AcONH_4$) was then increased from 15% to 30%, 50% and 55%, leading to a significant improvement of the peak shapes of AHLs with long side-chain (Fig. S1). The maximum percentage of co-solvent at 55% was finally kept for 4 min to elute all AHLs bearing side-chain longer than C16. The nature of the co-solvent was also studied by replacing the mixture MeOH/EtOH 1:1 (v/v) by pure MeOH, pure EtOH, EtOH/2-propanol mixture (1:1, v/v) and pure 2-propanol. The MeOH resulted in longer retention times (Fig. S2). Thus only EtOH, the EtOH/2-propanol mixture and 2-propanol were kept for further study using $AcONH_4$ additive at different concentrations. Fig. 3 shows the influence of the concentration of $AcONH_4$ additive (a) as well as the nature of co-solvent (b) on the signal of C18-HSL and C18:1-Δ^9-*cis*-HSL. EtOH with 50 mM $AcONH_4$ was finally selected since it offered a good peak geometry and the best sensitivity. Additionally, ethanol is considered as one of the greener solvent for environment. During these steps, the flow rate of the mobile phase was slightly increased from 1 to 1.1 $mL.min^{-1}$ leading to thinner peaks and a column pressure lower than 500 bar.

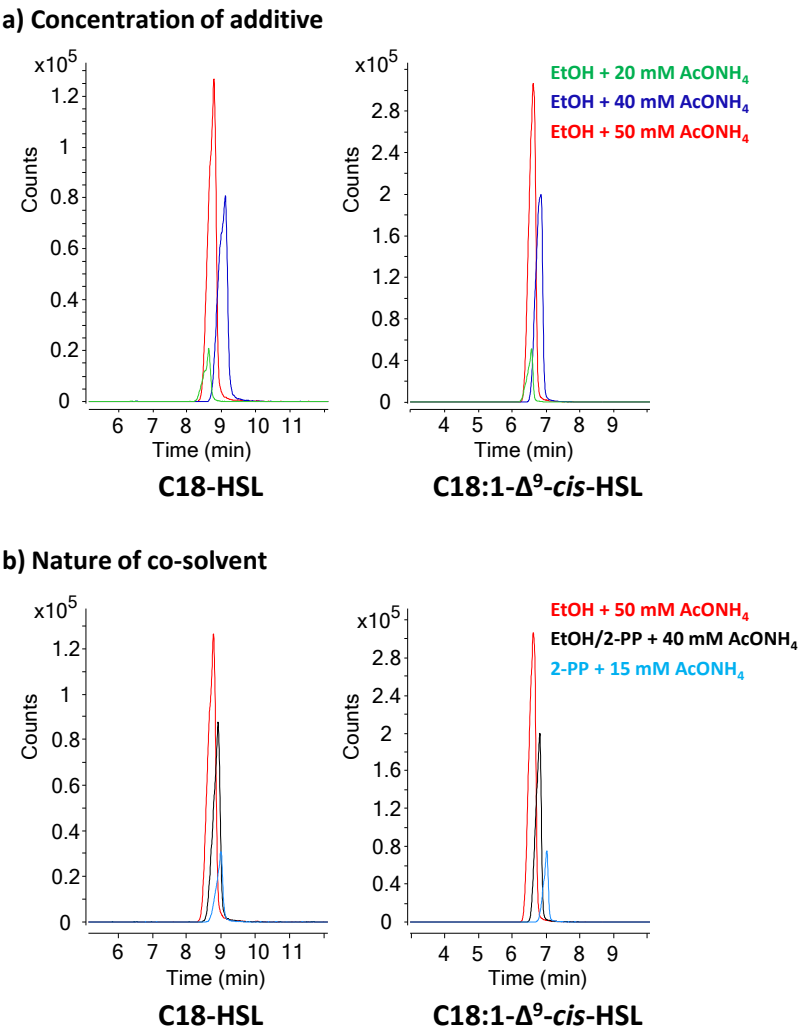

Fig. 3 Influence of the concentration of $AcONH_4$ additive added in EtOH using as co-solvent (a) and the nature of co-solvent represented by using EtOH, EtOH/2-PP 1:1 (v/v) and 2-PP at maximum concentration of $AcONH_4$ additive (b) on the signal of C18-HSL and C18:1-Δ^9-*cis*-HSL (2-PP = 2-propanol)

Next optimization step is related to the oven temperature which was screened from 30 to 60 °C by 10 °C step. The modification of temperature can change the state and the density of the mobile phase and as a result, it will change the retention time, the peak shape, as well as the sensibility of the method. When the oven temperature was increased, retention time of short side-chain AHLs (C6-HSLs to C8-HSLs) increased while that of long-chain AHLs (C15-HSLs to C18-HSLs) decreased as in case of two C18-HSLs showed in Fig. 4a. Furthermore, setting oven temperature at 60 °C offered a better sensitivity and finner chromatographic peak for all analytes. It must be also noted that high temperature decreases the column pressure that is crucial for column life time. The temperature of the column was therefore kept at 60 °C. The next step was to optimize the back-pressure regulator (BPR) setting. Four levels of the BPR were studied including 110, 130, 140 and 150 bar. The results show that the BPR at 140 and 150 bar gave a better sensitivity for all analytes without significant influence on peak geometry as showing in Fig. 4b for the C18-HSLs. The BPR at 140 bar was thus selected as being optimum avoiding system overpressure.

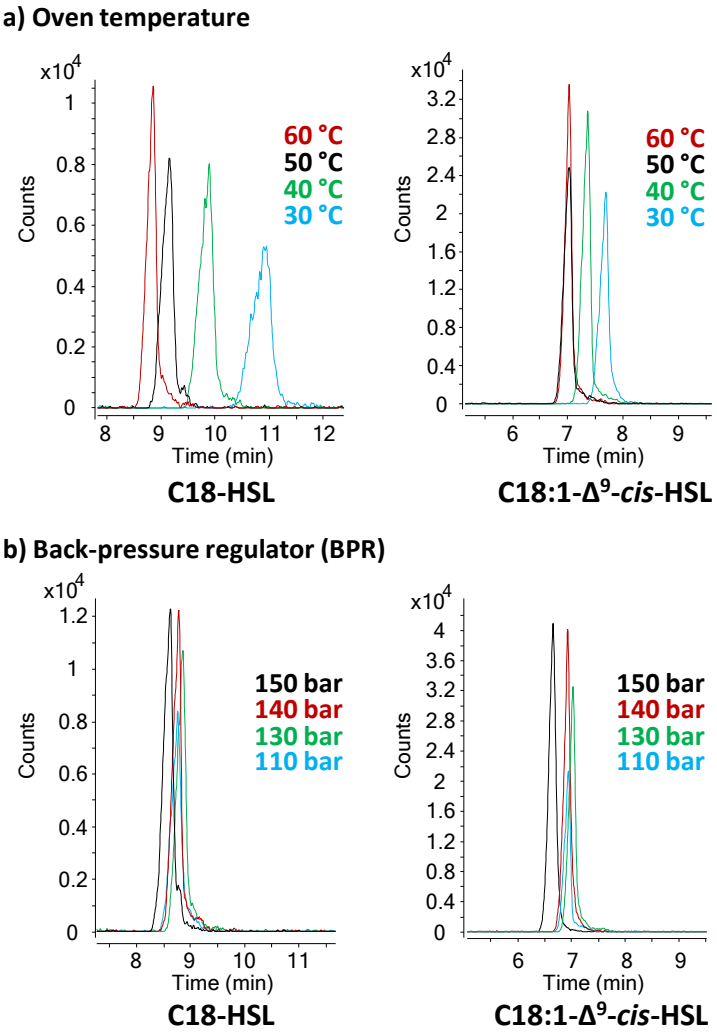

Fig. 4 Influence of the oven temperature (a) and the back-pressure regulator (b) on the signal of C18-HSL and C18:1-Δ^9-*cis*-HSL

Optimization of Ionization Parameters

Optimization of ionization settings was performed to reach the best sensitivity and to minimize in source fragmentation [28]. Three parameters were studied including the fragmentor voltage, the vaporizer temperature and the capillary voltage. It should be noted that the fragmentor voltage and the capillary voltage are compound-dependent parameters. The fragmentor voltage was tested with four values 80, 100, 120 and 150 V (Fig. 5a). At 150 V, a decrease of the ion peak intensity was observed for all AHLs, especially for the short side-chain AHLs, due to significant in source fragmentation leading to the detection of a typical fragment ion at *m/z* 102. The fragmentor voltage at 120 V offered a better sensitivity for all AHLs. The drying-gas temperature was then tested at 250, 300 and 350 °C (Fig. 5b). The result obtained at 350 °C shown higher peak intensity for all tested AHLs. This value was thus kept as optimum. Finally, capillary voltages at 2500, 3000 and 3500 V were investigated (Fig. 5c). Data show a peak intensity increase when increasing capillary voltage. A value of 3500 V for the capillary voltage was therefore selected.

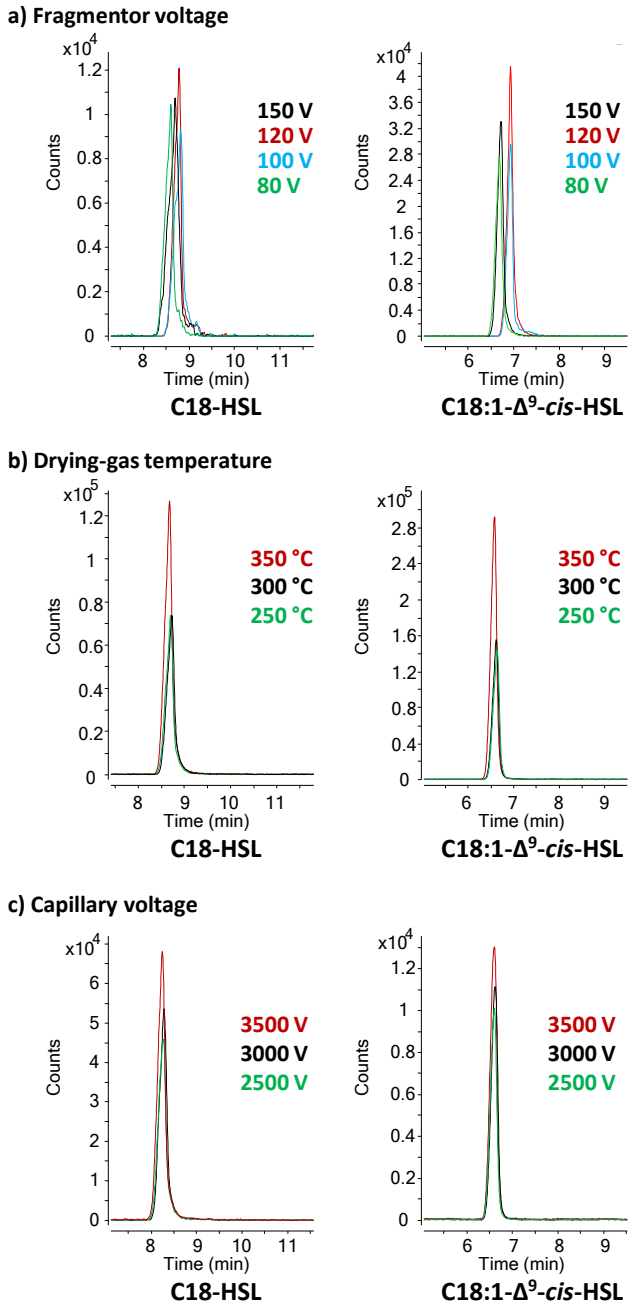

Fig. 5 Influence of the fragmentor voltage (a), the drying-gas temperature (b) and the capillary voltage (c) on the signal of C18-HSL and C18:1-Δ^9-*cis*-HSL

The mixture of 30 homoserine lactones was finally analyzed using these optimized conditions (Fig. 6). Isobaric AHLs or AHLs bearing a mass difference of 2 amu were separated at the baseline avoiding deconvolution of isotopic pattern for quantification. Concerning the order of elution, for AHLs having the same side-chain length, the 3-oxo-HSLs were eluted at the first, then non-substituted AHLs and finally the 3-OH-HSLs. The AHLs showing unsaturated side-chains were always eluted before those with saturated side-chain for the same number of carbon. This clearly indicates the good selectivity of the Hypercard™ column in separating AHL family. AHLs with short acyl side-chains, *i.e.* less than 14 carbons, led to symmetric and sharp chromatographic peaks within a retention time shorter than 5 min except for *N*-(*p*-Coumaroyl)-HSL.

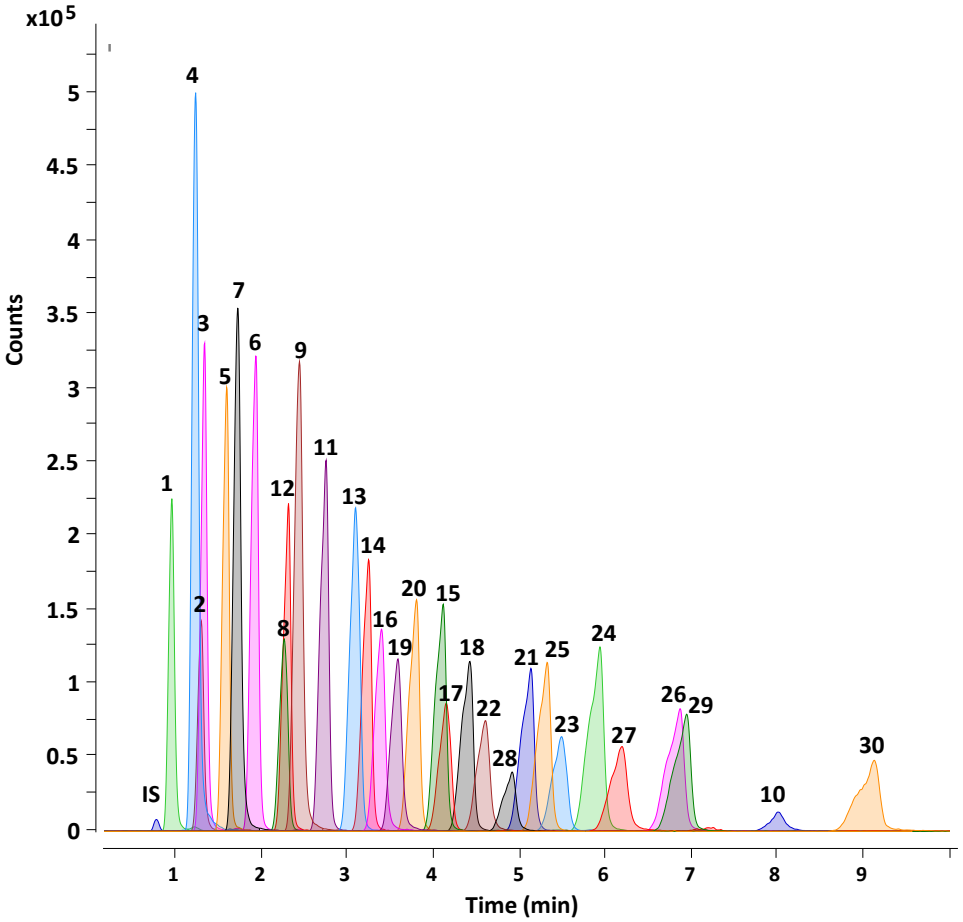

Fig. 6 Extracted ion chromatogram of 30 homoserine lactones analyzed by SFC-HRMS after optimization: The stationary phase was Hypercarb kept at 60 °C; the co-solvent was EtOH with 50 mM $AcONH_4$ (IS=internal standard, the number above chromatographic peak corresponding to the homoserine lactone number presented in Table 1)

Method Validation: Reproducibility, Method Linearity and Sensitivity

The quantification of homoserine lactones can be performed based on the peak area of the pseudo-molecular ion $[M+H]^+$ or the lactone ring fragment at *m/z* 102.055 which is characteristic for this class of compounds [10]. Under our established SFC-MS conditions, the protonated pseudo-molecular ion was always the most intense peak for all AHL standards and no interference was detected. The AHL quantification was therefore performed based on the signal of the protonated pseudo-molecular ion.

Table 1 Calibration curves and limits of quantification and detection for 30 homoserine lactones by SFC-HRMS (No. = Compound number; LOD = limit of detection; LOQ = limit of quantification)

No.	AHL	Molecular formula	$[M+H]^+$ theorical	Linearity					
				Slope and *y*-intercept	Coefficient of determination (R^2)	LOD		LOQ	
						µg.L^{-1}	pg	µg.L^{-1}	pg
1	C4-HSL	$C_8H_{13}NO_3$	172.0974	$y = 2.504x + 0.0402$	$R^2 = 0.9997$	2.02	2.42	16.1	19.4
2	3-OH-C4-HSL	$C_8H_{13}NO_4$	188.0923	$y = 1.3417x + 0.0921$	$R^2 = 0.9994$	4.03	4.84	16.1	19.4
3	C6-HSL	$C_{10}H_{17}NO_3$	200.1288	$y = 2.5982x + 0.2043$	$R^2 = 0.9989$	8.06	9.68	53.8	64.5
4	3-oxo-C6-HSL	$C_{10}H_{15}NO_4$	214.1079	$y = 3.7204x + 0.147$	$R^2 = 0.9997$	2.69	3.23	8.06	9.68
5	C7-HSL	$C_{11}H_{19}NO_3$	214.1443	$y = 2.1906x + 0.0273$	$R^2 = 0.9998$	4.03	4.84	22.5	27,0
6	C8-HSL	$C_{12}H_{21}NO_3$	228.1600	$y = 2.5407x - 0.0092$	$R^2 = 0.9993$	2.58	3.09	10.4	12.5
7	3-oxo-C8-HSL	$C_{12}H_{19}NO_4$	242.1392	$y = 2.896x - 0.0081$	$R^2 = 0.9991$	2.69	3.23	8.68	10.4
8	3-OH-C8-HSL	$C_{12}H_{21}NO_4$	244.1548	$y = 1.2423x + 0.0235$	$R^2 = 0.9997$	8.06	9.68	53.8	64.5
9	C9-HSL	$C_{13}H_{23}NO_3$	242.1756	$y = 1.717x + 0.0438$	$R^2 = 0.9998$	3.23	3.87	32.3	38.7
10	*N*-(*p*-Coumaroyl)-HSL	$C_{13}H_{13}NO_4$	248.0923	$y = 0.1973x - 0.0729$	$R^2 = 0.9976$	227	272	673	807
11	C10-HSL	$C_{14}H_{25}NO_3$	256.1913	$y = 2.0634x - 0.0408$	$R^2 = 0.9992$	4.03	4.84	32.3	38.7
12	3-oxo-C10-HSL	$C_{14}H_{23}NO_4$	270.1705	$y = 2.6523x + 0.0381$	$R^2 = 0.9997$	3.23	3.87	32.3	38.7
13	3-OH-C10-HSL	$C_{14}H_{25}NO_4$	272.1862	$y = 2.5054x - 0.0182$	$R^2 = 0.9992$	4.03	4.84	16.1	19.4
14	C11-HSL	$C_{15}H_{27}NO_3$	270.2069	$y = 1.7059x - 0.0134$	$R^2 = 0.9996$	4.03	4.84	32.3	38.7
15	C12-HSL	$C_{16}H_{29}NO_3$	284.2226	$y = 1.7075x + 0.0057$	$R^2 = 0.9997$	4.98	5.98	32.3	38.7
16	3-oxo-C12-HSL	$C_{16}H_{27}NO_4$	298.2018	$y = 1.5651x + 0.696$	$R^2 = 0.9983$	80.6	96.8	322	387
17	3-OH-C12-HSL	$C_{16}H_{29}NO_4$	300.2175	$y = 1.0657x + 0.111$	$R^2 = 0.9995$	53.8	64.6	161	194
18	C13-HSL	$C_{17}H_{31}NO_3$	298.2382	$y = 2.5583x + 0.0301$	$R^2 = 0.9998$	5.38	6.45	26.9	32.3
19	C14:1-Δ^9-*cis*-HSL	$C_{18}H_{31}NO_3$	310.2382	$y = 1.6696x + 0.0089$	$R^2 = 0.9995$	16.1	19.4	161	194
20	3-oxo-C14:1-Δ^7-*cis*-HSL	$C_{18}H_{29}NO_4$	324.2175	$y = 1.6865x - 0.03$	$R^2 = 0.9998$	16.1	19.4	80.6	96.8
21	C14-HSL	$C_{18}H_{33}NO_3$	312.2538	$y = 1.3605x + 0.0059$	$R^2 = 0.9995$	8.06	9.68	53.7	64.5
22	3-oxo-C14-HSL	$C_{18}H_{31}NO_4$	326.2331	$y = 0.9133x + 0.034$	$R^2 = 0.9999$	16.1	19.4	71.5	85.8
23	3-OH-C14-HSL	$C_{18}H_{33}NO_4$	328.2488	$y = 0.9392x + 0.0054$	$R^2 = 0.9998$	16.1	19.4	80.6	96.8
24	C15-HSL	$C_{19}H_{35}NO_3$	326.2695	$y = 2.5916x + 0.0085$	$R^2 = 0.9998$	5.38	6.45	35.8	43.0
25	C16:1-Δ^9-*cis*-HSL	$C_{20}H_{35}NO_3$	338.2695	$y = 1.3592x + 0.0193$	$R^2 = 0.9997$	32.3	38.7	80.6	96.8
26	C16-HSL	$C_{20}H_{37}NO_3$	340.2852	$y = 2.6391x + 0.0413$	$R^2 = 1.0000$	16.1	19.4	40.3	48.4
27	3-oxo-C16-HSL	$C_{20}H_{35}NO_4$	354.2644	$y = 0.9027x - 0.0003$	$R^2 = 0,9979$	161	194	806	968
28	3-oxo-C16:1-Δ^{11}-*cis*-HSL	$C_{20}H_{33}NO_4$	352.2488	$y = 0.3926x + 0.0841$	$R^2 = 0.9987$	35.2	42.2	161	194
29	C18:1-Δ^9-*cis*-HSL	$C_{22}H_{39}NO_3$	366.3008	$y = 1.2336x + 0.0033$	$R^2 = 0.9998$	32.3	38.7	80.6	96.8
30	C18-HSL	$C_{22}H_{41}N_3O$	368.3165	$y = 1.3913x - 0.0133$	$R^2 = 0.9998$	35.8	43.0	108	129

No chromatographic peak at *m/z* value and retention time of AHL standards were detected in pure acetonitrile suggesting the specificity of the methods. Table 1 displays the linear regressions, the slopes, the *y*-intercepts and the determination coefficients (R^2) for all AHL standards. The linearity was calculated over three orders of magnitude of concentration. The results show excellent linearity of the method with R^2 values better than 0.998. The coefficients of variation (%CV) were lower than 5% for all analytes at different levels of concentration showing the high reproducibility of the method. Calibration curves were conducted

at six-points of concentration for all AHLs except for *N*-(*p*-Coumaroyl)-HSL and 3-oxo-C12-HSL because of higher limits of quantification. The limits of detection (LODs) and the limits of quantification (LOQs) were calculated (Table 1) leading to LOD between 2 to 272 pg injected while LOQ between 10 to 968 pg injected.

Table 2 Results of intraday recovery, intra- and inter-day precision and accuracy of 30 homoserine lactones by SFC-HRMS (RSD = relative standard deviation, L = Low concentration, M = Medium concentration, H = High concentration, D = Day)

AHL	Intraday recovery RSD (%)		Intraday (n=3)						Interday (n=3)					
			Precision RSD (%)			Accuracy (%)			Precision RSD (%)			Accuracy (%)		
	L	H	H	M	L	H	M	L	D1	D2	D3	D1	D2	D3
C4-HSL	75.3	95.8	1.1	3.0	0.3	96.2	106.3	98.3	2.7	4.0	2.0	105.0	112.8	115.8
3-OH-C4-HSL	40.3	61.5	2.3	1.7	5.6	94.8	103.3	96.7	3.3	6.0	3.0	107.2	111.2	113.1
C6-HSL	73.6	101.7	0.6	1.2	2.3	97.1	92.4	100.6	3.6	5.1	3.1	108.1	107.7	112.1
3-oxo-C6-HSL	44.3	56.3	0.6	3.5	1.7	97.8	104.8	99.6	2.3	6.0	2.8	105.4	104.7	108.1
C7-HSL	73.1	94.1	2.5	4.4	2.6	97.3	104.3	97.9	2.3	7.5	2.3	103.7	104.2	108.2
C8-HSL	68.5	98.6	2.8	3.4	3.2	97.0	98.8	100.6	3.7	3.2	1.3	102.7	101.1	104.1
3-oxo-C8-HSL	44.7	65.5	2.9	3.6	2.1	100.5	100.6	104.7	2.4	8.4	3.4	105.3	107.1	109.0
3-OH-C8-HSL	78.3	95.0	2.2	2.9	2.5	95.9	95.2	99.6	2.9	2.0	4.2	102.8	103.4	103.6
C9-HSL	79.8	100.0	3.0	3.8	1.6	97.0	103.0	101.1	4.3	6.0	1.4	102.0	113.3	110.6
N-(*p*-Coumaroyl)-HSL		53.6	2.4	6.8	11.0	101.5	113.3	110.5	4.0	12.6	7.9	101.8	89.6	100.5
C10-HSL	74.2	97.3	1.3	4.6	3.0	95.1	104.3	100.1	0.3	7.5	0.9	101.1	109.3	115.2
3-oxo-C10-HSL	54.9	72.7	2.7	4.7	0.8	100.6	104.3	100.5	1.9	4.1	2.0	102.1	104.9	114.4
3-OH-C10-HSL	71.0	96.4	1.8	3.2	1.8	96.7	102.7	102.3	0.9	4.4	4.7	102.4	104.2	108.9
C11-HSL	71.0	99.6	3.6	5.6	6.8	94.2	102.7	103.6	0.5	5.9	5.2	101.2	106.5	113.3
C12-HSL	71.5	97.9	2.2	0.1	0.05	96.8	91.7	99.1	3.8	4.0	4.6	101.8	97.4	100.0
3-oxo-C12-HSL	60.9	75.4	3.0	3.1	6.7	107.2	87.4	85.6	3.0	1.1	1.7	85.0	92.5	98.7
3-OH-C12-HSL	71.7	96.3	1.4	2.8	5.6	98.7	95.2	99.8	3.5	2.7	2.9	100.3	100.5	99.3
C13-HSL	70.2	99.6	3.9	2.8	2.5	95.6	98.8	108.2	4.3	5.2	5.3	102.6	101.7	111.7
C14:1-Δ^9-*cis*-HSL	81.3	99.1	1.2	2.6	2.6	97.5	105.3	99.4	0.6	6.8	0.5	103.3	104.6	113.7
3-oxo-C14:1-Δ^7-*cis*-HSL	54.6	78,0	2.9	0.8	0.8	100.2	101.3	100.0	2.4	0.8	0.9	96.7	103.5	103.4
C14-HSL	79.6	100.7	2.8	4.6	2.0	96.9	103.4	99.7	4.9	4.4	1.8	103.1	107.2	114.7
3-oxo-C14-HSL	66.1	86.1	3.3	5.9	4.0	104.6	104.5	113.2	4.2	5.6	4.2	102.9	111.3	117.2
3-OH-C14-HSL	85.9	101.7	3.4	4.7	3.0	98.2	99.8	101.5	3.3	2.8	2.1	102.0	103.2	113.8
C15-HSL	72.9	99.5	3.5	3.4	1.6	100.1	101.8	98.2	4.7	5.3	2.3	101.8	104.9	113.1
C16:1-Δ^9-*cis*-HSL	70.7	93.3	0.9	5.6	3.0	98.4	104.8	102.9	1.9	5.7	2.5	101.5	104.3	113.4
C16-HSL	76.2	94.2	3.8	4.5	2.3	99.2	103.4	105.6	1.8	5.5	5.2	100.9	103.8	108.7
3-oxo-C16-HSL	42.7	86,0	3.8	3.2	0.3	98.9	97.4	99.6	3.6	3.2	0.3	96.1	95.6	102.7
3-oxo-C16:1-Δ^{11}-*cis*-HSL	56.9	74.7	4.9	6.7	12.3	115.0	102.6	103.7	3.4	4.8	1.0	102.5	105.2	113.8
C18:1-Δ^9-*cis*-HSL	74.8	97.1	4.6	8.5	6.4	98.8	95.2	107.1	2.6	1.5	0.5	101.8	87.5	95.3
C18-HSL	76.6	97.2	1.7	6.8	5.7	99.1	96.7	106.6	2.2	6.5	2.9	102.7	102.7	114.0

Results of intra- and inter-day precisions and accuracies are presented in Table 2. The intra-day precisions performed at three concentrations ranged between 0.05% and 12.3% and almost RSD values were lower

than 5% suggesting a good precision of the method. Intra-day accuracies were between 85.6% and 115.0%. Concerning inter-day results achieved at medium concentration, the precisions ranged from 0.3% to 12.6%, and inter-day accuracies were between 85.0% and 117.2%. These results suggest the good repeatability and reproducibility of the method.

The recovery of the extraction of 30 AHLs from the culture medium at two concentrations is given in Table 2. Recovery values were in the range of 40-86% for the low level and better recoveries from 54-102% were observed at a high level. The extraction recoveries of 3-oxo-HSLs were lower than those of non-substituted and 3-OH-HSLs. *N*-(*p*-Coumaroyl)-HSL showed a low extraction recovery of 54% at high concentration whereas it was not detected at the low level because of its limit of quantification.
These results confirm the sensitivity, precision and accuracy of the method making it suitable for quantitative profiling of AHLs.

Identification and Quantification of AHLs Produced by *Paraburkholderia* sp. BSNB-0670 Strain

The validated method was applied to identify the AHLs in the extract of one gram-negative endophytic bacterium *Paraburkholderia* sp. BSNB-0670 [22]. The genus *Paraburkholderia* consists of non-pathogenic and beneficial species, which were found in diverse ecological niches [29, 30]. Some species belonging to this genus are described as having an AHL-based QS system, designated BraI/R which responses to 3-oxo-C14-HSL [31]. Furthermore, this QS system found in *P. phymatum* was also shown to produce various long side-chain AHLs [32]. The extraction of *Paraburkholderia* sp. BSNB-0670 was performed using CH_2Cl_2 to have an exhaustive recovery of AHLs with long side-chain as well as to avoid the hydrolysis of AHLs. Among 30 AHL standards used for method validation, 19 known AHLs were detected according to their retention time ($\Delta t_R < 0.25$ min) and the exact mass measurement. This strain abundantly produces 3-oxo-HSLs and 3-OH-HSLs. Nine 3-oxo-HSLs and 3-OH-HSLs were quantified and the results are shown in Table 3. Ten AHLs were detected as a trace amount in which the C15-HSL was detected in very low quantity resulting in a low mass accuracy (> 10 ppm).

Further study on uncommon AHLs produced by the *Paraburkholderia* sp. BSNB-0670 strain was considered. In order to annotate signals as AHLs, SFC-MS/MS data obtained using a data-dependent acquisition (DDA) mode were preprocessed by MZmine 2 [23] leading to the calculation of a molecular network (MN) by MetGem software [25]. The obtained MN containing 55 nodes is shown in Fig. 6. The AHLs are expected to be clustered according to similar fragmentation pattern of the lactone part leading to fragment ions at *m/z* 102, 84, 74 and 56 [10].

Table 3 Identification and quantification of AHLs produced by *Paraburkholderia* sp. BSNB-0670

Number	Identified AHL	Molecular formula	Theoretical *m/z**	Observed *m/z*	Δ ppm	Δt_R min	Concentration $mg.L^{-1}$
3	C6-HSL	$C_{10}H_{17}NO_3$	200.1288	200.1294	3.0	0.03	NQ
4	3-oxo-C6-HSL	$C_{10}H_{15}NO_4$	214.1079	214.1077	-0.9	0.00	0.43±0.04
5	C7-HSL	$C_{11}H_{19}NO_3$	214.1443	214.1444	0.5	-0.05	NQ
6	C8-HSL	$C_{12}H_{21}NO_3$	228.1600	228.1601	0.4	0.01	NQ
7	3-oxo-C8-HSL	$C_{12}H_{19}NO_4$	242.1392	242.1392	0.0	0.04	1.36±0.11
8	3-OH-C8-HSL	$C_{12}H_{21}NO_4$	244.1548	244.1549	0.4	0.02	1.17±0.03
9	C9-HSL	$C_{13}H_{23}NO_3$	242.1756	242.1755	-0.4	-0,07	NQ
12	3-oxo-C10-HSL	$C_{14}H_{23}NO_4$	270.1705	270.1705	0.0	0.02	3.05±0.13
13	3-OH-C10-HSL	$C_{14}H_{25}NO_4$	272.1862	272.1864	0.7	0.00	2.89±0.15
14	C11-HSL	$C_{15}H_{27}NO_3$	270.2069	270.2062	-2.6	-0.15	NQ
15	C12-HSL	$C_{16}H_{29}NO_3$	284.2226	284.2224	-0.7	-0.01	NQ
16	3-oxo-C12-HSL	$C_{16}H_{27}NO_4$	298.2018	298.2019	0.3	0.03	8.53±0.17
17	3-OH-C12-HSL	$C_{16}H_{29}NO_4$	300.2175	300.2175	0.0	0.25	18.96±0.47
20	3-oxo-C14:1-Δ^7-*cis*-HSL	$C_{18}H_{29}NO_4$	324.2175	324.217	-1.5	0.00	NQ
21	C14-HSL	$C_{18}H_{33}NO_3$	312.2538	312.254	0.6	-0.02	NQ
22	3-oxo-C14-HSL	$C_{18}H_{31}NO_4$	326.2331	326.2332	0.3	-0.04	1.33±0.02
23	3-OH-C14-HSL	$C_{18}H_{33}NO_4$	328.2488	328.2487	-0.3	-0.11	1.66±0.03
24	C15-HSL	$C_{19}H_{35}NO_3$	326.2695	326.273	10.7	-0.11	NQ
26	C16-HSL	$C_{20}H_{37}NO_3$	340.2852	340.2857	1.5	-0.11	NQ

*Theoretical *m/z* corresponds to the pseudo-molecular ion $[M+H]^+$

NQ: non quantificable; t_R: retention time

All detected AHLs clustered together in a single cluster. Nine abundant AHLs including four OH-HSLs in green and five oxo-HSLs in dark-red were well separated into two subgroups. Two ions at *m/z* 316.2126 and 298.2025 had the same retention time and were different by 18.0101 Da corresponding to a water loss suggesting that the ion at *m/z* 298.2025 was a fragment product of the ion at *m/z* 316.2126. The predicted molecular formula of the protonated molecule at *m/z* 298.2025 is $C_{16}H_{27}NO_4$ with 2.3 ppm of mass error. This ion was linked to the 3-OH-HSL subgroup and exhibits a retention time higher than that of 3-oxo-C12-HSL. We can thus postulate that the ion at *m/z* 298.2025 is corresponding to 3-OH-C12:1-HSL, which was not described previously in the literature. However, it is very complex to determine the position of the double bond based only on the MS/MS data in this case. It should be noted that during the extraction and analysis process, no water was used. The ion at *m/z* 316.2126 could correspond to the 3-OH-C12:1-HSL with an opened lactone ring, which would be a product of the natural hydrolysis of the lactone ring observed in some bacteria as described in the article of Patel *et al.* [10]. This study also proposed characteristic fragment ions which permitted to determine AHL hydrolysis including the significant appearance of the ion at *m/z* 120.065. However, this fragment ion was not found in the MS/MS spectrum of the ion *m/z* 316.2126 (Fig. S4), suggesting that the ion at *m/z* 316.2126 was that of a 3,n-diOH-C12:0-HSL*, i.e.*, a C12-HSL with two hydroxyl groups on the side-chain. Three protonated molecules at *m/z* 296.186 belong to the 3-oxo-HSL

subgroup for two of them and to the 3-OH-HSL subgroup for the last one. This is confirmed by their retention time order. A chemical formula $C_{16}H_{25}NO_4$ can be proposed for these three molecules with 0.3 and 1.4 ppm of mass error for *m/z* 296.1861 and 296.1866, respectively. The two ions eluted at 3.83 and 4.02 min were suggested as two isomers of 3-oxo-C12:1-HSL and the other one eluted at 5.55 min can be attributed to 3-OH-C12:2-HSL. In the literature, only the 3-oxo-C12:1-Δ^5-*cis*-HSL was isolated from a marine *Mesorhizobium* sp. together with other long-chain AHLs [33]. The 3-OH-C12:2-HSL was never described before. It should be noted that, besides the quorum-sensing activity, C12-HSL analogs presented some interesting biological activities such as 3-oxo-C12-HSL which induced various immunostimulatory activities in host cells [34, 35] and apoptosis in macrophages and neutrophils [36, 37]. The 3-oxo-C12:1-Δ^5-*cis*-HSL was also described to induce the antibacterial activity and the cytotoxicity against some tumor cell lines [33]. The 3-oxo-C12:2-HSL isolated from the gut microbiome of inflammatory bowel disease patients was also briefly reported in a congress as having anti-inflammatory properties but no effect on paracellular permeability contrary to 3-oxo-C12-HSL [38]. However, the isolation as well as the structural determination of this compound were not described.

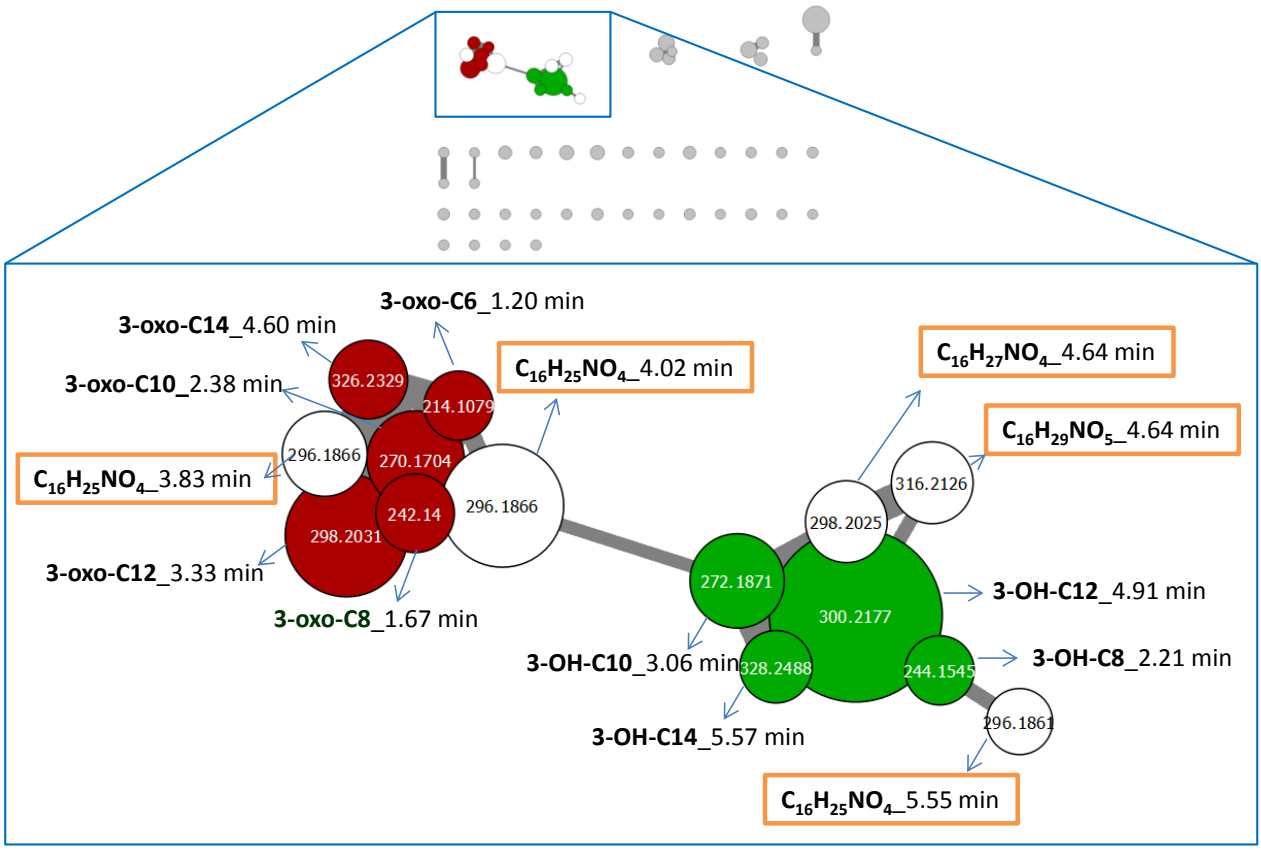

Fig. 6 MS/MS molecular networking of a CH_2Cl_2 extract of *Paraburkholderi*a sp. BSNB-0670 obtained by SFC-HRMS/MS analysis with their identification

Conclusions

A rapid and sensitive method for the simultaneous quantification of up to 30 AHLs by SFC-HRMS was developed and validated. The limit of detection and quantification of AHLs in this present method were in the same order of magnitude as that described in the literature by using LC-MS/MS [10, 15, 16]. The

advantage of this method was focused on the utilization of CO_2 and EtOH as the mobile phase so it is considered as a "green" method. Furthermore, by comparing the retention time of AHLs analyzed by SFC-MS and that analyzed by LC-MS [10], our method permits to save analysis time with a factor of two.
This method was successfully applied to determine AHLs produced by *Paraburkholderia* sp. BSNB-0670. The molecular network based on SFC-HRMS/MS data allowed to annotate four unknown C12-HSL. It will be interesting to carry out large-scale cultivation of the BSNB-0670 strain to purify and elucidate the structure of these C12-HSLs as well as evaluate their biological activity. These results contribute to confirm the efficiency of SFC-HRMS/MS in the analysis of the natural product.

Acknowledgments

This work was supported by the Agence Nationale de la Recherche (Grant ANR-16-CE29-0002-01 CAP-SFC-MS), "Investissement d'Avenir" grant managed by Agence Nationale de la Recherche (CEBA, ref ANR-10-LABX-25-01), a joint Agence Nationale de la Recherche - Swiss National Science Foundation (ANR-SNF) grant (SECIL, ref ANR-15-CE21-0016 and SNF N° 310030E-164289) and a grant from Région Ile-de-France (DIM Analytics).

Conflict of Interest

The authors declare no conflict of interest.

References

1. Williams P. Quorum sensing, communication and cross-kingdom signalling in the bacterial world. Microbiology. 2007;153(Pt 12):3923-38.
2. Fuqua WC, Winans SC, Greenberg EP. Quorum sensing in bacteria: the LuxR-LuxI family of cell density-responsive transcriptional regulators. J Bacteriol. 1994;176(2):269-75.
3. Williams P, Winzer K, Chan W, Cámara M. Look who's talking: communication and quorum sensing in the bacterial world. Philos Trans R Soc, B. 2007;362(1483):1119-34.
4. von Bodman SB, Willey JM, Diggle SP. Cell-cell communication in bacteria: united we stand. J Bacteriol. 2008;190(13):4377-91.
5. González JF, Venturi VT. A novel widespread interkingdom signaling circuit. Trends Plant Sci. 2013;18(3):167-74.
6. Sperandio V. Novel approaches to bacterial infection therapy by interfering with bacteria-to-bacteria signaling. Expert Rev Anti-Infect Ther. 2007;5(2):271-6.
7. Càmara M, Daykin M, Chhabra SR. Detection, purification, and synthesis of *N*-acyl homoserine lactone quorum sensing signal molecules. Methods Microbiol. 1998;27:319-30.
8. Doberva M, Stien D, Sorres J, Hue N, Sanchez-Ferandin S, Eparvier V et al. Large diversity and original structures of acyl-homoserine lactones in strain MOLA 401, a marine *Rhodobacteraceae* bacterium. Front Microbiol 2017;8:1152.
9. Wang Y, Zhang X, Wang C, Fu L, Yi Y, Zhang Y. Identification and quantification of acylated homoserine lactones in *Shewanella baltica*, the specific spoilage organism of *Pseudosciaena crocea*, by ultrahigh-performance liquid chromatography coupled to triple quadrupole mass spectrometry. J Agric Food Chem. 2017;65(23):4804-10.
10. Patel NM, Moore JD, Blackwell HE, Amador-Noguez D. Identification of unanticipated and novel *N*-Acyl L-Homoserine Lactones (AHLs) using a sensitive non-targeted LC-MS/MS method. PLoS One. 2016;11(10):e0163469.
11. Steindler L, Venturi V. Detection of quorum-sensing *N*-acyl homoserine lactone signal molecules by bacterial biosensors. FEMS Microbiol Lett. 2007;266(1):1-9.

12. Cataldi TR, Bianco G, Frommberger M, Schmitt-Kopplin P. Direct analysis of selected *N*-acyl-L-homoserine lactones by gas chromatography/mass spectrometry. Rapid Commun Mass Spectrom. 2004;18(12):1341-4.
13. Charlton TS, de Nys R, Netting A, Kumar N, Hentzer M, Givskov M et al. A novel and sensitive method for the quantification of *N*-3-oxoacyl homoserine lactones using gas chromatography-mass spectrometry: application to a model bacterial biofilm. Environ Microbiol. 2000;2(5):530-41.
14. Frommberger M, Hertkorn N, Englmann M, Jakoby S, Hartmann A, Kettrup A et al. Analysis of *N*-acylhomoserine lactones after alkaline hydrolysis and anion-exchange solid-phase extraction by capillary zone electrophoresis-mass spectrometry. Electrophoresis. 2005;26(7-8):1523-32.
15. Ortori CA, Dubern JF, Chhabra SR, Cámara M, Hardie K, Williams P et al. Simultaneous quantitative profiling of *N*-acyl-L-homoserine lactone and 2-alkyl-4(1*H*)-quinolone families of quorum-sensing signaling molecules using LC-MS/MS. Anal Bioanal Chem. 2011;399(2):839-50.
16. Purohit AA, Johansen JA, Hansen H, Leiros HK, Kashulin A, Karlsen C et al. Presence of acyl-homoserine lactones in 57 members of the *Vibrionacea*e family. J Appl Microbiol. 2013;115(3):835-47.
17. Leipert J, Treitz C, Leippe M, Tholey A. Identification and quantification of *N*-acyl homoserine lactones involved in bacterial communication by small-scale synthesis of internal standards and matrix-assisted laser desorption/ionization mass spectrometry. J Am Soc Mass Spectrom. 2017;28(12):2538-47.
18. Laboureur L, Bonneau N, Champy P, Brunelle A, Touboul D. Structural characterisation of acetogenins from *Annona muricata* by supercritical fluid chromatography coupled to high-resolution tandem mass spectrometry. Phytochem Anal. 2017;28(6):512-20.
19. He PX, Zhang Y, Zhou Y, Li GH, Zhang JW, Feng XS. Supercritical fluid chromatography-a technical overview and its applications in medicinal plant analysis: an update covering 2012-2018. Analyst. 2019.
20. West C. Current trends in supercritical fluid chromatography. Anal Bioanal Chem 2018;410(25):6441-57.
21. Liu LX, Zhang Y, Zhou Y, Li GH, Yang GJ, Feng XS. The application of supercritical fluid chromatography in food quality and food safety: An overview. Crit Rev Anal Chem. 2019:1-25.
22. Barthélemy M, Elie N, Pellissier L, Wolfender JL, Stien D, Touboul D et al. Structural identification of antibacterial lipids from Amazonian palm tree endophytes through the molecular network approach. Int J Mol Sci. 2019;20(8):E2006.
23. Pluskal T, Castillo S, Villar-Briones A, Oresic M. MZmine 2: modular framework for processing, visualizing, and analyzing mass spectrometry-based molecular profile data. BMC Bioinf. 2010;11:395.
24. Myers OD, Sumner SJ, Li S, Barnes S, Du X. One step forward for reducing false positive and false negative compound identifications from mass spectrometry metabolomics data: New algorithms for constructing extracted ion chromatograms and detecting chromatographic peaks. Anal Chem. 2017;89(17):8696-703.
25. Olivon F, Elie N, Grelier G, Roussi F, Litaudon M, Touboul D. MetGem software for the generation of molecular networks based on the t-SNE algorithm. Anal Chem. 2018;90(23):13900-8.
26. MacDougall D, Amore FJ, Cox GV, Crosby DG, Estes FL, Freeman DH et al. Guidelines for data acquisition and data quality evaluation in environmental chemistry. Anal Chem. 1980;52:2242–9.
27. West C, Lesellier E. Orthogonal screening system of columns for supercritical fluid chromatography. J Chromatogr A 2008;1203(1):105-13.
28. Riddell N, Bavel B, Jogsten IE, McCrindle R, McAlees A, Chittim B. Coupling supercritical fluid chromatography to positive ion atmospheric pressure ionization mass spectrometry: ionization optimization of halogenated environmental contaminants. Int J Mass Spectrom. 2017;421:156–63.
29. Sawana A, Adeolu M, Gupta RS. Molecular signatures and phylogenomic analysis of the genus *Burkholderia*: proposal for division of this genus into the emended genus *Burkholderia* containing pathogenic organisms and a new genus *Paraburkholderia* gen. nov. harboring environmental species. Front Genet. 2014;5:429.
30. Coenye T, Vandamme P. Diversity and significance of *Burkholderia* species occupying diverse ecological niches. Environ Microbiol. 2003;5(9):719-29.
31. Suárez-Moreno ZR, Caballero-Mellado J, Venturi V. The new group of non-pathogenic plant-associated nitrogen-fixing *Burkholderia* spp. shares a conserved quorum-sensing system, which is tightly regulated by the RsaL repressor. Microbiology. 2008;154(Pt 7):2048-59.

32. Coutinho BG, Mitter B, Talbi C, Sessitsch A, Bedmar EJ, Halliday N et al. Regulon studies and in planta role of the BraI/R quorum-sensing system in the plant-beneficial *Burkholderia* cluster. Appl Environ Microbiol. 2013;79(14):4421-32.
33. Krick A, Kehraus S, Eberl L, Riedel K, Anke H, Kaesler I et al. A marine *Mesorhizobium* sp. produces structurally novel long-chain *N*-acyl-L-homoserine lactone. Appl Environ Microbiol. 2007;73(11):3587-94.
34. DiMango E, Zar HJ, Bryan R, Prince A. Diverse *Pseudomonas aeruginosa* gene products stimulate respiratory epithelial cells to produce interleukin-8. J Clin Invest. 1995;96(5):2204-10.
35. Smith RS, Kelly R, Iglewski BH, Phipps RP. The Pseudomonas autoinducer *N*-(3-oxododecanoyl) homoserine lactone induces cyclooxygenase-2 and prostaglandin E2 production in human lung fibroblasts: implications for inflammation. J Immunol. 2002;169(5):2636-42.
36. Tateda K, Ishii Y, Horikawa M, Matsumoto T, Miyairi S, Pechere JC et al. The *Pseudomonas aeruginosa* autoinducer *N*-3-oxododecanoyl homoserine lactone accelerates apoptosis in macrophages and neutrophils. Infect Immun. 2003;71(10):5785-93.
37. Horikawa M, Tateda K, Tuzuki E, Ishii Y, Ueda C, Takabatake T et al. Synthesis of *Pseudomonas* quorum-sensing autoinducer analogs and structural entities required for induction of apoptosis in macrophages. Bioorg Med Chem Lett. 2006;16(8):2130-3.
38. Le Balc'h E, Landman C, Tauziet E, Brot L, Quevrain E, Rainteau D et al.. 3-oxo-C12:2-HSL, a new *N*-acyl-homoserine lactone identified in gut ecosystem exerts an anti-inflammatory effect and does not modify paracellular permeability. The 12th Congress of ECCO – European Crohn's and Colitis Organisation; 2017; Barcelona.